Eur. Phys. J. A **23**, 435–443 (2005)
DOI 10.1140/epja/i2004-10113-x

THE EUROPEAN PHYSICAL JOURNAL A

A test of the zero-range DWBA method at astrophysical energies

A. Adahchour[a] and P. Descouvemont[b]

Physique Nucléaire Théorique et Physique Mathématique, CP 229, Université Libre de Bruxelles, B-1050 Brussels, Belgium

Received: 19 August 2004 / Revised version: 29 November 2004 /
Published online: 12 January 2005 –
Communicated by V. Vento

Abstract. The DWBA method is tested through a comparison with a microscopic cluster model on the $^{13}\mathrm{C}(\alpha,\mathrm{n})^{16}\mathrm{O}$ reaction in the energy range $E = 0$–$5\,\mathrm{MeV}$, relevant for nuclear astrophysics. The conditions of the calculation are as close as possible to the reference model, *i.e.* the nucleus-nucleus potentials are phase equivalent, and the spectroscopic factors are identical. We find significant differences between both approaches, which means that antisymmetrization effects, missing in the DWBA, are important. Our work also points out the strong sensitivity of the DWBA with input parameters.

PACS. 24.10.-i Nuclear reaction models and methods – 24.10.Eq Coupled-channel and distorted-wave models

1 Introduction

The Distorted-Wave Born Approximation (DWBA) method is widely used in nuclear physics and in nuclear astrophysics [1–4]. It essentially deals with transfer reactions and relies upon the knowledge of nucleus-nucleus potentials in the entrance and exit channels, as well as of the spectroscopic factors of the colliding nuclei. In nuclear astrophysics [5], the DWBA is usually used for two purposes. On one hand, the low-energy transfer cross-section can be derived if the nucleus-nucleus potentials and the spectroscopic factors are available. The difficulty of measuring the cross-sections down to stellar energies makes theoretical models such as the DWBA useful tools to complement experimental data. Applications to reactions such as $^{7}\mathrm{Li}(\mathrm{p},\alpha)^{4}\mathrm{He}$ [6], $^{19}\mathrm{F}(\mathrm{p},\alpha)^{16}\mathrm{O}$ [7] or $^{10}\mathrm{B}(\mathrm{p},\alpha)^{7}\mathrm{Be}$ [8] have been investigated by the DWBA method.

On the other hand, the DWBA is used to analyze energy spectra or to determine spectroscopic factors. A typical example is the $^{20}\mathrm{Ne}(^{3}\mathrm{He},\mathrm{t})^{20}\mathrm{Na}$ which provided the low-energy spectrum of $^{20}\mathrm{Na}$ with spin and parity assignments [9]. A further advantage associated with this technique is the high value of transfer cross-sections, compared to capture cross-sections. This property is crucial for reactions involving radioactive elements, since current intensities are rather low.

The main disadvantage of the DWBA is the need for parameters which are poorly known, or not known at all. This essentially occurs in reactions involving radioactive nuclei where the interacting potentials should be adapted from neighboring reactions. In addition, the spectroscopic factors are expected to be somewhat dependent on the potentials. A recent work by Keeley *et al.* [10] highlights some difficulties related to DWBA calculations. Their analysis of the $^{13}\mathrm{C}(^{6}\mathrm{Li},\mathrm{d})^{17}\mathrm{O}$ data by Kubono *et al.* [11] contradicts the original analysis performed by the authors of ref. [11]. Keeley *et al.* mention possible uncontrolled parameters in the DWBA approach.

The aim of this work is to test the DWBA by comparing it with results provided by a microscopic cluster model [12]. In this model, the cross-sections only depend on a nucleon-nucleon interaction, and on some assumptions about the cluster structure of the colliding nuclei. Spectroscopic factors are naturally included. Consequently the predictive power of a microscopic model is rather strong, and it is an ideal starting point for a test of the DWBA. In this work, we limit ourselves to the zero-range approximation, which enables a significant simplification of the DWBA formalism, and is often used in the literature. The zero-range approximation is known to be accurate for light particles, such as nucleons or α-particles [2,3].

The comparison is done for the $^{13}\mathrm{C}(\alpha,\mathrm{n})^{16}\mathrm{O}$ reaction which is quite important in astrophysics as the main neutron source, and which has been analyzed in a microscopic model [13]. We limit ourselves to low energies,

[a] *Permanent address*: LPHEA, FSSM, Université Caddi Ayyad, Marrakech, Morocco.
[b] Directeur de Recherches FNRS; e-mail: pdesc@ulb.ac.be

which are relevant for nuclear astrophysics, and where absorption channels can be neglected. We apply the DWBA with conditions of the calculation as close as possible to those of the microscopic model. In other words, the $\alpha + {}^{13}\mathrm{C}$ and $\mathrm{n} + {}^{16}\mathrm{O}$ potentials are fitted on the microscopic phase shifts, and the spectroscopic factors are taken from the model. Then the comparison of the microscopic and DWBA ${}^{13}\mathrm{C}(\alpha,\mathrm{n})^{16}\mathrm{O}$ transfer cross-section will provide an estimate of the accuracy of the DWBA.

We apply the DWBA in different conditions, simulated by different partial waves of the ${}^{13}\mathrm{C}(\alpha,\mathrm{n})^{16}\mathrm{O}$ reaction. A non-resonant partial wave represents the natural application, as the DWBA is essentially aimed at describing direct reactions. However, at low energies, and in light systems, reactions involving a broad resonance can be approximately considered as a direct process. We therefore extend our work to partial waves involving a broad resonance, or a subthreshold state Let us notice that the ${}^{13}\mathrm{C}(\alpha,\mathrm{n})^{16}\mathrm{O}$ reaction is just an example to test the DWBA. Although its importance in astrophysics is well established, we do not aim here at deriving any astrophysical data.

A further investigation will be done by analyzing the sensitivity of the DWBA cross-section with respect to the nucleus-nucleus potentials. As microscopic models use completely antisymmetric wave functions, this comparison should give an information on how important antisymmetrization effects are in transfer reactions. A similar analysis has been performed for capture reactions in ref. [14], and shows that antisymmetrization effects are not negligible, even at low energies.

The DWBA is based on the assumption that the transfer process is weak with respect to the dominant elastic channel. Below the Coulomb barrier, the physical origin of this smallness is essentially due to the penetration factor, which strongly reduces the cross-section. At 3 MeV, *i.e.* near or slightly above the Coulomb barrier, the experimental cross-section is about 10 mb [15] which, assuming an isotropic process, corresponds to a differential transfer cross-section $\mathrm{d}\sigma_t/\mathrm{d}\Omega \approx 1\,\mathrm{mb/sr}$. Data for elastic cross-sections [16] show a non-negligible anisotropy, but a rough estimate of the elastic cross-section provides $\mathrm{d}\sigma_{\mathrm{el}}/\mathrm{d}\Omega \approx 200\,\mathrm{mb/sr}$. This strong reduction factor of the transfer cross-section, even near the Coulomb barrier, supports the applicability of the DWBA.

In sect. 2, we briefly present the DWBA formalism, by considering different types of reactions: exchange, stripping and knock-out. The application to the ${}^{13}\mathrm{C}(\alpha,\mathrm{n})^{16}\mathrm{O}$ cross-section in presented in sect. 3. Section 4 is devoted to concluding remarks and outlook.

2 The DWBA method

2.1 Introduction

The DWBA formalism has been developed in many papers (see for example ref. [4] and references therein). Here we limit ourselves to basic formulas, and use the so-called "channel-spin representation" [4] which is well suited to a comparison with microscopic results. Most works use a different coupling mode, exhibiting the transferred angular momentum. In the present case, the spin of the colliding nuclei are first coupled to the channel spin S, which in turn is coupled to the orbital momentum L to provide the total spin of the system J. This coupling mode is well adapted to reactions involving resonances, essentially characterized by their spin and parity.

Let us assume two colliding nuclei A and a, with spins I_A and I_a in the entrance channel. The asymptotic behavior of the wave function is given by

$$\Psi_\alpha^{M_A M_a}(\boldsymbol{k}_\alpha, \boldsymbol{r}_\alpha) \longrightarrow \Phi^{I_A M_A}\Phi^{I_a M_a} \exp(i\boldsymbol{k}_\alpha.\boldsymbol{r}_\alpha), \quad (1)$$

where we neglect the Coulomb interaction. In (1), M_A and M_a are the spin projections, $\boldsymbol{r}_\alpha$ is the relative distance and $\boldsymbol{k}_\alpha$ the wave number; the internal wave functions are denoted as $\Phi^{I_A M_A}$ and $\Phi^{I_a M_a}$ and implicitly depend on internal coordinates. Specific cases, such as exchange or stripping reactions, will be considered in the next subsections.

In the presence of an interaction between particles A and a, a partial-wave expansion of the scattering wave function (1) gives

$$\Psi_\alpha^{M_A M_a}(\boldsymbol{k}_\alpha, \boldsymbol{r}_\alpha) = \frac{4\pi}{k_\alpha r_\alpha} \sum_{L_\alpha S_\alpha J M \pi} \langle L_\alpha m_\alpha S_\alpha M_\alpha | J M\rangle \times \left[\Phi^{I_A} \otimes \Phi^{I_a}\right]^{S_\alpha M_\alpha} \chi^{J\pi}_{L_\alpha S_\alpha}(r_\alpha) Y^{m_\alpha}_{L_\alpha}(\hat{r}_\alpha) Y^{m_\alpha \star}_{L_\alpha}\left(\hat{k}_\alpha\right), \quad (2)$$

where $\chi^{J\pi}_{L_\alpha S_\alpha}(r_\alpha)$ is a partial wave in the entrance channel, and π is the total parity $\pi = (-1)^{L_\alpha}\pi_A\pi_a$. According to ref. [4], the scattering amplitude for a transition from channel α to channel β is given by

$$A^{M_A M_a, M_B M_b}_{\beta\alpha}(\boldsymbol{k}_\alpha, \boldsymbol{k}_\beta) = -\frac{(\mu_\alpha\mu_\beta)^{1/2}}{2\pi\hbar^2}\left(\frac{k_\beta}{k_\alpha}\right)^{1/2} \times \left\langle \Psi^{M_B M_b (-)}_\beta(\boldsymbol{k}_\beta, \boldsymbol{r}_\beta)\middle| V \middle|\Psi^{M_A M_a (+)}_\alpha(\boldsymbol{k}_\alpha, \boldsymbol{r}_\alpha)\right\rangle, \quad (3)$$

where μ_α and μ_β are the reduced masses and V the residual interaction. In the matrix element, integration is performed over all spatial coordinates. For the wave function in the final channel β, a development analogous to (2) is assumed, with $\Phi^{I_B M_B}$ and $\Phi^{I_b M_b}$ as internal wave functions of the residual nuclei. The collision matrix for a total spin J is defined as

$$U^{J\pi}_{L_\alpha S_\alpha, L_\beta S_\beta} = \delta_{L_\alpha L_\beta}\delta_{S_\alpha S_\beta} + \frac{ik_\alpha}{2\pi} \times \sum_{M_A M_a M_B M_b m_\alpha m_\beta} \langle L_\alpha m_\alpha S_\alpha M_\alpha | J M\rangle \langle L_\beta m_\beta S_\beta M_\beta | J M\rangle \times \langle I_A M_A I_a M_a | S_\alpha M_\alpha\rangle \langle I_B M_B I_b M_b | S_\beta M_\beta\rangle \times \iint \mathrm{d}\hat{k}_\alpha\, \mathrm{d}\hat{k}_\beta Y^{m_\alpha}_{L_\alpha}\left(\hat{k}_\alpha\right) Y^{m_\beta}_{L_\beta}\left(\hat{k}_\beta\right) A^{M_A M_a, M_B M_b}_{\beta\alpha}(\boldsymbol{k}_\alpha, \boldsymbol{k}_\beta). \quad (4)$$

The coupling scheme is chosen to show up the channel spins and angular momenta. This choice is well adapted

to the study of resonances, characterized by a total spin J. Using definition (3) of the scattering amplitude, we have

$$U^{J\pi}_{L_\alpha S_\alpha, L_\beta S_\beta} = \delta_{L_\alpha L_\beta}\delta_{S_\alpha S_\beta} - i\frac{(\mu_\alpha\mu_\beta k_\alpha k_\beta)^{1/2}}{(2\pi\hbar)^2} \times \iint \mathrm{d}r_\alpha\, \mathrm{d}r_\beta r_\alpha^2 r_\beta^2 W^{J\pi}_{\alpha\beta}(r_\alpha, r_\beta)\chi^{J\pi\star}_{L_\alpha S_\alpha}(r_\alpha)\chi^{J\pi}_{L_\beta S_\beta}(r_\beta), \quad (5)$$

with

$$W^{J\pi}_{\alpha\beta}(r_\alpha, r_\beta) = \frac{(4\pi)^2}{k_\alpha r_\alpha k_\beta r_\beta} \times \left\langle \left[[\Phi^{I_B}\otimes\Phi^{I_b}]^{S_\beta}\otimes Y_{L_\beta}(\hat{r}_\beta)\right]^J \times|V|\ \left[[\Phi^{I_A}\otimes\Phi^{I_a}]^{S_\alpha}\otimes Y_{L_\alpha}(\hat{r}_\alpha)\right]^J\right\rangle. \quad (6)$$

This matrix element is obtained after integration over $\hat{r}_\alpha$, $\hat{r}_\beta$ and over the internal coordinates. As usual, the collision matrix is parameterized as

$$U^{J\pi}_{L_\alpha S_\alpha, L_\beta S_\beta} = \epsilon^{J\pi}_{L_\alpha S_\alpha, L_\beta S_\beta}\exp\left(2i\delta^{J\pi}_{L_\alpha S_\alpha, L_\beta S_\beta}\right), \quad (7)$$

where ϵ is the transition amplitude and δ the phase shift. Definitions (5) and (6) are general. They are now developed for specific cases.

2.2 Exchange or knock-out reactions

In such reactions, the target nucleus A is assumed to be composed of a core nucleus C and the emitted particle b ($A = C + b$), whereas the residual nucleus B is comprised of the core and the projectile a ($B = C + a$). This reaction is written as

$$a + A\,(= C + b) \longrightarrow b + B\,(= C + a), \quad (8)$$

and is illustrated in fig. 1. An example is the $^{13}\mathrm{C}(\alpha,\mathrm{n})^{16}\mathrm{O}$ reaction where the α-particle and the neutron are exchanged during the reaction; ^{12}C is the core nucleus.

The internal coordinates are $\boldsymbol{r}_{bC}$ and $\boldsymbol{r}_{aC}$, which should be converted in $\boldsymbol{r}_\alpha$ and $\boldsymbol{r}_\beta$. The relationships between the $(\boldsymbol{r}_{bC}, \boldsymbol{r}_{aC})$ and $(\boldsymbol{r}_\alpha, \boldsymbol{r}_\beta)$ systems are given by

$$\boldsymbol{r}_{bC} = \left(\boldsymbol{r}_\beta + \frac{a}{B}\boldsymbol{r}_\alpha\right)\Big/\left(1 - \frac{ab}{AB}\right)$$
$$\boldsymbol{r}_{aC} = \left(\boldsymbol{r}_\alpha + \frac{b}{A}\boldsymbol{r}_\beta\right)\Big/\left(1 - \frac{ab}{AB}\right), \quad (9)$$

and the Jacobian is

$$J = \left[\frac{AB}{C(B+b)}\right]^3.$$

According to eq. (8), the internal wave functions of nuclei A and B are defined as

$$\Phi^{I_A M_A} = \mathcal{C}_A\sqrt{\mathcal{S}_A}u_{\ell_b}(r_{bC})\left[Y_{\ell_b}(\hat{r}_{bC})\otimes\Phi^{I_b}\right]^{I_A M_A}, \quad (10)$$

where $\mathcal{S}_A$ is the spectroscopic factor, $\mathcal{C}_A$ is the isospin Clebsch-Gordan coefficient, and $u_{\ell_b}(r_{bC})$ is a radial wave function related to the $C + b$ system. For the sake of simplicity we assume here that the core nucleus has a spin zero. A similar definition holds for the residual nucleus B:

$$\Phi^{I_B M_B} = \mathcal{C}_B\sqrt{\mathcal{S}_B}u_{\ell_a}(r_{aC})\left[Y_{\ell_a}(\hat{r}_{aC})\otimes\Phi^{I_a}\right]^{I_B M_B}. \quad (11)$$

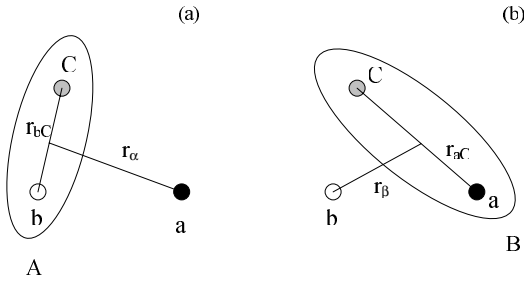

Fig. 1. Scheme of the exchange reaction (see eq. (8)). (a) Before the reaction, (b) after the reaction.

To compute the matrix element (6) we must specify the residual interaction V. As we are mainly interested in a qualitative comparison between the DWBA and a microscopic approach, we use here the zero-range approximation, which allows an important simplification of the calculation. Generalization to finite-range approaches can be found in refs. [3,4] for example, but they are presented in a different coupling mode. In the zero-range approximation, the interaction potential between the exchanged particles a and b is written as

$$V(\boldsymbol{r}_{ab}) = V_0\delta(\boldsymbol{r}_{aC} - \boldsymbol{r}_{bC}) = V_0\left(\frac{B+b}{B}\right)^3\delta\left(\boldsymbol{r}_\beta - \frac{A}{B}\boldsymbol{r}_\alpha\right), \quad (12)$$

where we have used eqs. (9). This potential contains a central term only, and neglects spin-orbit or tensor contributions.

In the zero-range approximation, the matrix element (6) is obtained after some angular-momentum algebra; we have

$$W^{J\pi}_{\alpha\beta}(r_\alpha, r_\beta) = 4\pi V_0\mathcal{C}_A\mathcal{C}_B\frac{(\mathcal{S}_A\mathcal{S}_B)^{1/2}}{k_\alpha k_\beta r_\alpha r_\beta}\left(\frac{A}{C}\right)^3 u_{\ell_a}\left(\frac{A}{C}r_\alpha\right) \times u_{\ell_b}\left(\frac{A}{C}r_\alpha\right)\delta\left(r_\beta - \frac{A}{B}r_\alpha\right) \times \sum_{I_{ab},\lambda}\hat{I}_{ab}\hat{\lambda}Z^J_{I_{ab},\lambda}(\ell_a, L_\beta, S_\beta, I_a, I_b, I_B) \times Z^J_{I_{ab},\lambda}(\ell_b, L_\alpha, S_\alpha, I_b, I_a, I_A), \quad (13)$$

where coefficient Z is defined as

$$Z^J_{I_{ab},\lambda}(\ell_a, L_\beta, S_\beta, I_a, I_b, I_B) = (-1)^{L_\beta}\left[\hat{L}_\beta\hat{S}_\beta\hat{I}_B\right]^{1/2} \times\langle L_\beta 0\lambda 0|\ell_a 0\rangle\begin{Bmatrix}\ell_a & I_a & I_B\\ I_b & S_\beta & I_{ab}\end{Bmatrix}\begin{Bmatrix}I_{ab} & \ell_a & S_\beta\\ L_\beta & J & \lambda\end{Bmatrix}, \quad (14)$$

and where we have introduced the notation $\hat{x} = 2x + 1$. In eq. (14), I_{ab} results from the coupling of spins I_a and I_b

and λ corresponds to the transferred angular momentum. If we assume $I_a = \ell_b = 0$, eq. (13) is strongly simplified, and reduces to

$$W^{J\pi}_{\alpha\beta}(r_\alpha, r_\beta) = 4\pi V_0 \mathcal{C}_A \mathcal{C}_B \frac{(\mathcal{S}_A \mathcal{S}_B)^{1/2}}{k_\alpha k_\beta r_\alpha r_\beta} \left(\frac{A}{C}\right)^3 u_0\left(\frac{A}{C} r_\alpha\right) \times u_{\ell_a}\left(\frac{A}{C} r_\alpha\right) \delta\left(r_\beta - \frac{A}{B} r_\alpha\right) \left[\hat{L}_\alpha \hat{L}_\beta \hat{S}_\beta\right]^{1/2} \times (-1)^{L_\alpha + L_\beta + \ell_a + S_\beta + J} \times \langle L_\beta 0 L_\alpha 0 | \ell_a 0\rangle \begin{Bmatrix} I_b & \ell_a & S_\beta \\ L_\beta & J & L_\alpha \end{Bmatrix}. \quad (15)$$

This expression has been used to determine the ^{13}C$(\alpha, \mathrm{n})^{16}$O cross-section, presented in sect. 3.

2.3 Stripping reactions

A reaction such as ^{13}C$(\alpha, \mathrm{n})^{16}$O can be seen in two different ways: i) the α and neutron are exchanged or ii) a ^{3}He particle is stripped from α to the ^{13}C target. In general a stripping reaction $A(a, b)B$ is assumed to occur with a projectile made up of the emitted particle b and another particle x which is captured by the target. The stripping process is illustrated in fig. 2. The interaction responsible is usually taken as $V(r_{bx})$, the interaction potential between particles b and x. We need to specify the matrix element (6) for stripping reactions.

The relationships between the $(\boldsymbol{r}_{bC}, \boldsymbol{r}_{aC})$ and $(\boldsymbol{r}_\alpha, \boldsymbol{r}_\beta)$ systems are now given by

$$\boldsymbol{r}_{Ax} = \frac{bAB}{ax(A+a)} \boldsymbol{r}_\beta - \left(1 + \frac{bA^2}{ax(A+a)}\right) \boldsymbol{r}_\alpha$$
$$\boldsymbol{r}_{bx} = \frac{AB}{x(A+a)} \left(\boldsymbol{r}_\beta - \frac{A}{B} \boldsymbol{r}_\alpha\right), \quad (16)$$

and the Jacobian is

$$J = \left[\frac{AB}{x(A+a)}\right]^3.$$

As before, the wave functions of particles a and B are defined as

$$\Phi^{I_a M_a} = \mathcal{C}_a \sqrt{\mathcal{S}_a} u_{\ell_a}(r_{bx}) \left[Y_{\ell_a}(\hat{r}_{bx}) \otimes \Phi^{I_{bx}}\right]^{I_a M_a},$$
$$\Phi^{I_B M_B} = \mathcal{C}_B \sqrt{\mathcal{S}_B} u_{\ell_B}(r_{Ax}) \left[Y_{\ell_B}(\hat{r}_{Ax}) \otimes \Phi^{I_{Ax}}\right]^{I_B M_B}, \quad (17)$$

where I_{bx} and I_{Ax} result from the couplings of I_b and I_x, and of I_A and I_x, respectively. As for exchange reactions, we use the zero-range approximation [2],

$$V(\boldsymbol{r}_{bx}) u_{\ell_a}(r_{bx}) Y_{\ell_a}(\hat{r}_{bx}) = D_0 \delta(\boldsymbol{r}_{bx}) = D_0 \left[\frac{AB}{x(A+a)}\right]^{-3} \delta\left(\boldsymbol{r}_\beta - \frac{A}{B} \boldsymbol{r}_\alpha\right), \quad (18)$$

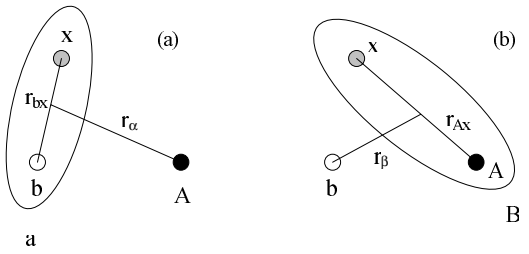

Fig. 2. Scheme of the stripping reaction. (a) Before the reaction, (b) after the reaction.

which selects s waves only for ℓ_a. With this approximation, the matrix element (6) is

$$W^J_{\alpha\beta}(r_\alpha, r_\beta) = 4\pi D_0 \frac{\mathcal{C}_a \mathcal{C}_B (\mathcal{S}_a \mathcal{S}_B)^{1/2}}{k_\alpha k_\beta r_\alpha r_\beta} \times u_{\ell_B}(r_\alpha) \delta\left(r_\beta - \frac{A}{B} r_\alpha\right) (-1)^{I_{Ax} + I_a + I_b + L_\alpha + J + I_A + S_\alpha} \times \left[\hat{\ell}_B \hat{L}_\beta \hat{I}_B \hat{S}_\alpha \hat{S}_\beta \hat{I}_{Ax} \hat{I}_a\right]^{1/2} \langle \ell_B 0 L_\beta 0 | L_\alpha 0\rangle \times \begin{Bmatrix} \ell_B & I_B & I_{Ax} \\ I_b & S_\alpha & S_\beta \end{Bmatrix} \begin{Bmatrix} \ell_B & L_\beta & L_\alpha \\ J & S_\alpha & S_\beta \end{Bmatrix} \begin{Bmatrix} I_A & I_x & I_{Ax} \\ I_b & S_\alpha & I_a \end{Bmatrix}. \quad (19)$$

For the ^{13}C$(\alpha, \mathrm{n})^{16}$O reaction, we have

$$I_A = I_B = 0,$$
$$I_a = I_x = I_b = 1/2,$$

and eq. (19) is simplified to

$$W^J_{\alpha\beta}(r_\alpha, r_\beta) = 4\pi D_0 \frac{\mathcal{C}_a \mathcal{C}_B (\mathcal{S}_a \mathcal{S}_B)^{1/2}}{k_\alpha k_\beta r_\alpha r_\beta} \times u_{\ell_B}(r_\alpha) \delta\left(r_\beta - \frac{A}{B} r_\alpha\right) (-1)^{L_\alpha + J + 1/2} \left(\hat{L}_\beta \hat{\ell}_B / 2\right)^{1/2} \times \langle \ell_B 0 L_\beta 0 | L_\alpha 0\rangle \begin{Bmatrix} \ell_B & L_\alpha & L_\beta \\ J & 1/2 & 1/2 \end{Bmatrix}. \quad (20)$$

For a pick-up reaction, the cross-section is obtained in the same way, by swapping the roles of channels α and β.

3 Application to the ^{13}C$(\alpha, \mathrm{n})^{16}$O reaction

3.1 Outline of the microscopic model

In a microscopic model, the wave functions depend upon all nuclear coordinates, and are antisymmetrized to account for the Pauli principle. The cross-sections are derived from a A-body Hamiltonian which contains one or two parameters in the nucleon-nucleon interaction. As our reference calculation is based on a microscopic cluster model, we give here a brief description of this model. In a microscopic model [12,17], the Hamiltonian of the system reads

$$H = \sum_{i=1}^{A} T_i + \sum_{i<j}^{A} V_{ij}\,, \quad (21)$$

where A is the nucleon number, T_i the kinetic energy of nucleon i and V_{ij} an effective nucleon-nucleon interaction.

In the Resonating Group Method (RGM), a trial wave function of the A-nucleon system is defined from cluster wave functions ϕ_1 and ϕ_2. In RGM notations, the total wave function with the total angular momentum J and parity π is therefore

$$\Psi^{JM\pi} = \sum_{\alpha\ell I} \mathcal{A}\big[[\phi_1^\alpha \otimes \phi_2^\alpha]^I \otimes Y_\ell(\Omega)\big]^{JM} g^{J\pi}_{\alpha\ell I}(\rho), \quad (22)$$

where $\boldsymbol{\rho} = (\rho, \Omega)$ is the relative coordinate, $\mathcal{A}$ the A-nucleon antisymmetrization operator and I the channel spin. The relative functions $g^{J\pi}_{\alpha\ell I}(\rho)$ are to be determined from the Schrödinger equation of the system. Label α takes the values 1 and 2 for the $\alpha + {}^{13}$C and n $+ {}^{16}$O channels, respectively.

In practice, functions $g^{J\pi}_{\alpha\ell I}(\rho)$ are expanded over a Gaussian basis involving the Generator Coordinate R where the Gaussian functions are centred. This method is known as the Generator Coordinate Method (GCM —see refs. [12,18]), and allows a systematic treatment of the calculations. It has been applied to many systems, in recent years (see references in ref. [18]). In the GCM, wave function (22) is rewritten as

$$\Psi^{JM\pi} = \sum_{\alpha\ell I} \int f^{J\pi}_{\alpha\ell I}(R)\, \Phi^{JM\pi}_{\alpha\ell I}(R)\, \mathrm{d}R, \quad (23)$$

where $\Phi^{JM\pi}_{\alpha\ell I}(R)$ is a projected Slater determinant, and $f^{J\pi}_{\alpha\ell I}(R)$ the generator function. The calculation of the radial functions is therefore replaced by the calculation of the generator functions. The use of the R-matrix method provides a correct description of boundary conditions, and allows us to apply definition (23) for scattering states as well as for bound states.

3.2 Conditions of the calculation

The ^{13}C$(\alpha,$n$)^{16}$O reaction plays an important role in nuclear astrophysics [5]. It has been investigated by several groups (see ref. [11] and references therein), and is a good candidate to be studied by the DWBA method. Our goal here is not to provide an optimized DWBA analysis, but to test its precision and sensitivity through a comparison with a previous microscopic study [13]. In ref. [13], the cluster model was shown to provide a fair description of the available cross-sections; it also pointed out the importance of the $1/2^+_2$ subthreshold state in ^{17}O.

In the present work, we compare the transition amplitude ϵ (7) obtained in the microscopic model with the DWBA approach. We refer to ref. [13] for the conditions of the microscopic calculation. The transition amplitudes provide the transfer cross-section. We use, in the DWBA method, conditions as close as possible to those of ref. [13]. In other words, the $\alpha + {}^{13}$C and n $+ {}^{16}$O potentials, used to generate the radial wave functions χ (see eq. (5)) are determined by fitting the microscopic phase shifts. The Q value, taken from the literature [19], is $Q = 2.22$ MeV. The other ingredients of the DWBA are

Table 1. Spectroscopic factors $\mathcal{S}$.

System	$\mathcal{S}$	$\mathcal{C}$
^{13}C=^{12}C + n	1	1
^{16}O=^{12}C + α	0.33	1
^{4}He=^{3}He + n	1	$1/\sqrt{2}$
^{16}O=^{13}C + ^{3}He	0.19	$1/\sqrt{2}$

- The ^{12}C + n and ^{12}C + α wave functions u_0 in eqs. (15) and (20). In the microscopic theory, the ^{13}C and ^{16}O wave functions are defined in the shell model [12,13]. Accordingly, the ^{12}C + n and ^{12}C + α wave functions are harmonic-oscillator orbitals with angular momentum $\ell = 1\,(0)$, and number of radial nodes $n_r = 0\,(2)$ for ^{12}C + n (^{12}C + α).
- The spectroscopic factors of ^{13}C and ^{17}O, which are taken from the microscopic model. These are determined as explained in ref. [20], and are given in table 1.
- The amplitude V_0 of the α + n potential, assumed to have a zero range. This is determined by fitting an α + n equivalent potential on the microscopic phase shifts, and then by evaluating the volume integral. From eq. (12), we have

$$V_0 = 4\pi \int V_{\alpha+n}(r)\, r^2\, \mathrm{d}r. \quad (24)$$

  As is well known the α + n system presents a non-negligible parity effect. Averaging over both parities, we obtain $V_0 = -2700$ MeV fm^3.
- For stripping reactions we need the zero-range amplitude D_0. For the ^{3}He + n wave function, we assume a $0s$ oscillator function, which is consistent with the shell-model description of the α-particle used in the microscopic approach. For the ^{3}He + n potential, a Gaussian approximation has been used, with parameters constrained by the α binding energy. Different sets of potentials provide values between -900 and -1100 MeV fm$^{3/2}$. We have adopted $D_0 = -1000$ MeV fm$^{3/2}$.

The transition amplitude ϵ is then determined for some typical partial waves. We have chosen here $J^\pi = 1/2^+, 1/2^-$ and $3/2^-$, which present different behaviors: the $1/2^+$ partial wave involves a subthreshold state, $1/2^-$ a broad resonance near 2 MeV, and $3/2^-$ is non-resonant. In the ^{13}C$(\alpha,$n$)^{16}$O reaction, the main contribution comes from the $1/2^+$ partial wave. Although the resonant character of the process is accounted for in the wave functions, the validity of the DWBA for narrow resonance and for subthreshold states is less well established. In the literature, it has been applied both to non-resonant (see ref. [7] for example) and resonant (see refs. [8,21] for example) cross-sections. Let us remind that our main aim here is to compare the DWBA with a microscopic approach, in conditions typical of those found in the literature. The partial waves are chosen as a representative set of conditions occurring in low-energy reactions.

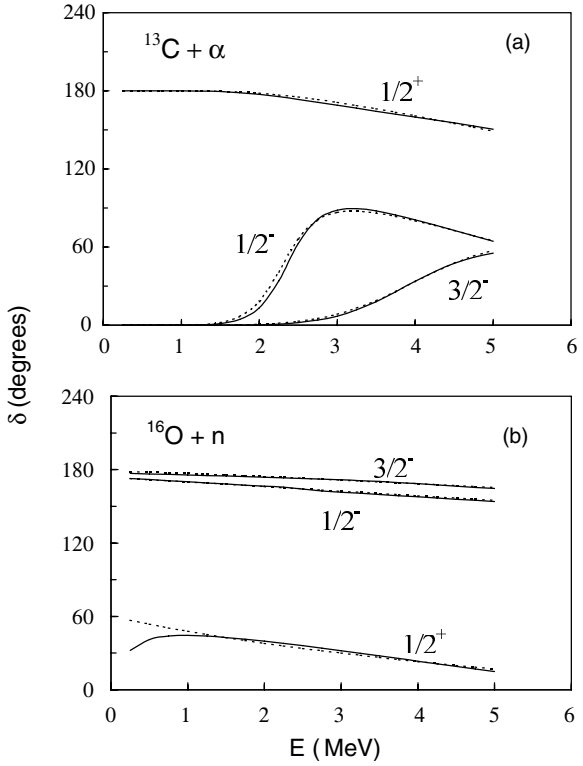

Fig. 3. Microscopic (solid lines) and potential-model (dotted lines) $\alpha + {}^{13}$C (a) and n + ^{16}O (b) phase shifts. Energies are expressed in the c.m. of the $\alpha + {}^{13}$C channel.

Table 2. Potential parameters (see eq. (25)). m_ℓ is the number of forbidden states. Potentials are in MeV and lengths in fm.

J	ℓ	V_1	a_1	V_2	a_2	m_ℓ
$^{13}\mathrm{C}+\alpha$						
$1/2^+$	1	−88.0	2.97	−160	1.0	3
$1/2^-$	0	−28.0	3.43	−500	1.0	3
$3/2^-$	2	−40.0	3.07	−500	1.0	2
$^{16}\mathrm{O}+\mathrm{n}$						
$1/2^+$	0	−77.0	2.36			1
$1/2^-$	1	−39.0	3.50			1
$3/2^-$	1	−50.0	3.15			1

3.3 Results assuming an exchange process

In this subsection, we assume that the $^{13}\mathrm{C}(\alpha,\mathrm{n})^{16}\mathrm{O}$ reaction proceeds through an exchange mechanism. The external neutron of ^{13}C and the incident α-particle are exchanged during the collision. An other assumption, *i.e.* the stripping of a ^{3}He fragment from the α-particle will be considered later. This comparison will be a further test of the sensitivity of the DWBA with respect to basic assumptions.

The $^{13}\mathrm{C}+\alpha$ and $^{16}\mathrm{O}+\mathrm{n}$ phase shifts are given in fig. 3. For the DWBA calculations, these phase shifts have been fitted by a Gaussian potential

$$V(r) = V_1 \exp\big(-(r/a_1)^2\big) + V_2 \exp\big(-(r/a_2)^2\big). \quad (25)$$

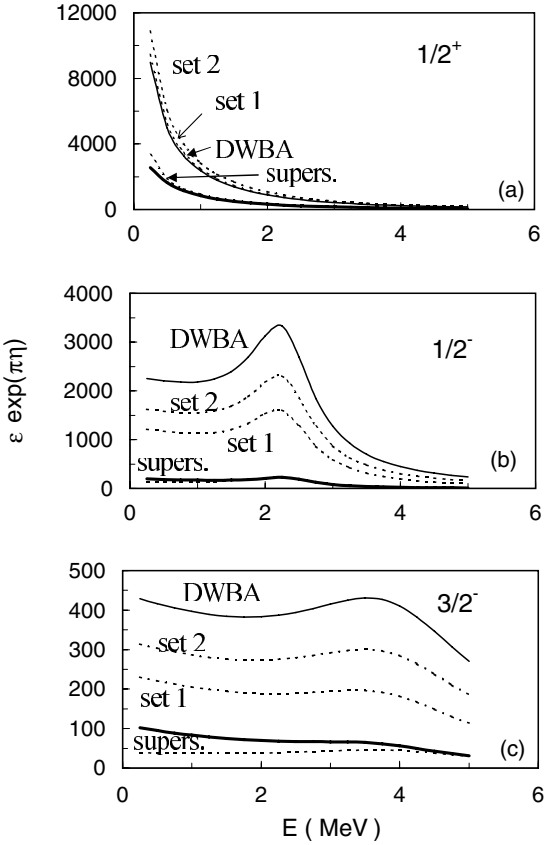

Fig. 4. Transition amplitudes obtained in the exchange approximation for $J = 1/2^+$ (a), $J = 1/2^-$ (b), and $J = 3/2^-$ (c). Thick curves: reference microscopic calculation, solid curves: DWBA calculation, dotted curves: DWBA calculation with modifications of the conditions of the calculation (see text).

The potential depths are chosen according to the number of forbidden states, which play an important role in microscopic theories [12]. Also the bound-state energies should be reproduced reasonably well by the nucleus-nucleus potentials. To this end, a single Gaussian function is not sufficient, and we need to introduce a second function in the potential. The parameters are given in table 2; these potentials reproduce the microscopic phase shifts within 2° or better. As we deal with low energies, absorption is negligible, and the potentials are therefore real. The system is composed of two channels with spin $\frac{1}{2}$; the collision matrix (7) is therefore of size (2×2), and for each partial wave a single transition amplitude ϵ is defined. It determines the coupling between the $^{13}\mathrm{C}+\alpha$ and $^{16}\mathrm{O}+\mathrm{n}$ channels.

The transition amplitudes ϵ are given in fig. 4. In order to remove the strong energy dependence occurring at subCoulomb energies, we have divided ϵ by the penetration factor $\exp(-\pi\eta)$, where η is the Sommerfeld parameter. Figure 4 shows that the DWBA does reproduce the energy dependence. This is not surprising since the energy dependence is mainly given by the wave functions in the entrance channel, which are derived from a phase-equivalent potential. The normalization, however,

Table 3. $^{12}C + n$ and $^{12}C + \alpha$ potentials, with the corresponding $\sqrt{\langle r^2 \rangle}$ values. Potentials are in MeV and lengths in fm.

	V_1	a_1	$\sqrt{\langle r^2 \rangle}$
$^{12}C + n$			
set 1	−80.4	2.10	2.74
set 2	−94.8	1.90	2.58
$^{12}C + \alpha$			
set 1	−100.0	2.56	2.90
set 2	−112.1	2.36	2.75

is somewhat different. The DWBA overestimates the reference calculation. The overestimation factor is about 4 for $J = 1/2^-$ and 2 for $J = 3/2^-$. For $J = 1/2^+$, the low-energy part is essentially determined by the properties of the $1/2^+$ subthreshold state, which yield the low-energy enhancement.

One of the main goals of the present work is to evaluate the sensitivity of the DWBA against some inputs. As a first test, we have replaced the harmonic-oscillator wave functions of ^{13}C and ^{16}O by more realistic functions, deduced from a potential model. This approach is not fully consistent with the microscopic model, but provides an interesting way to evaluate the DWBA stability. We have used single-Gaussian potentials with the parameters fitted to the experimental binding energies (−4.95 MeV for $^{12}C + n$ and −7.16 MeV for $^{12}C + \alpha$). Two different sets (see table 3) have been used. They slightly differ by the $\sqrt{\langle r^2 \rangle}$ values, *i.e.* the mean distance between ^{12}C and α or neutron. Figure 4 shows that the transition amplitude is rather sensitive to the ^{13}C and ^{16}O wave functions. These wave functions are very close to harmonic-oscillator functions, corresponding to the microscopic model, but the long-range part presents a more physical behavior, and slight changes in the inner part have a non-negligible effect on the transition amplitude.

A further test of the sensitivity of the DWBA has been performed by replacing the $^{13}C + \alpha$ and $^{16}O + n$ potentials by their supersymmetric partners. The supersymmetric transform [22] keeps the phase shifts unchanged, but deep potentials are replaced by equivalent potentials presenting a repulsive core. The corresponding wave functions do not have nodes associated with the forbidden states [22]. The results are shown in fig. 4, where we find out that the DWBA is much closer to the microscopic results. The DWBA appears to be quite sensitive to the description of the scattering wave functions (up to a factor of 20 for $J^\pi = 1/2^-$), although the phase shifts are identical. There is no physical argument to conclude that supersymmetric potentials are better adapted than deep potentials. Until now, different attempts (see, *e.g.*, refs. [23,24]) have been done to compare both approaches in different conditions such as spectroscopy [23] or nucleus-nucleus bremsstrahlung [24]. In these works, supersymmetric and deep potentials provide very similar results. This is not the case for the DWBA, but the better agreement obtained with supersymmetric potentials is probably a coincidence. Further studies are needed to clarify this conclusion.

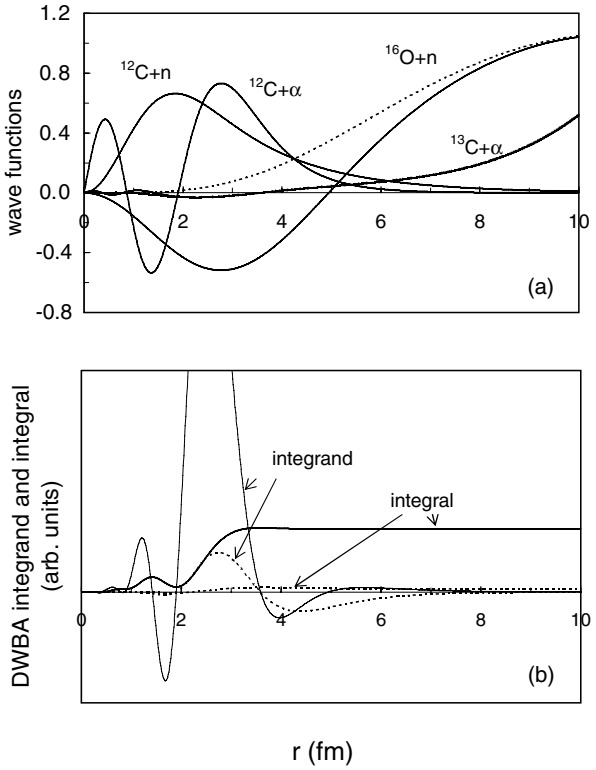

Fig. 5. Upper panel (a): $^{13}C + \alpha$ and $^{16}O + n$ wave functions for $J^\pi = 1/2^-$ and $E = 0.25$ MeV. Lower panel (b): integral (thick curve) and integrand (thin curve) (5). The supersymmetric results are given as dotted curves.

To understand this striking feature, we have analyzed the DWBA integral (5) in more detail. In fig. 5, we present the zero-range integrand (5) along with the integral up to a finite distance r. The calculation is done $J^\pi = 1/2^-$, and for 3 different energies; 0.25 MeV is a typical energy for astrophysical applications. As shown in fig. 5, the integrand presents fast variations at small distances ($r \leq 4$ fm). Only short distances contribute to the DWBA matrix element. Consequently, slight modifications in the wave functions have a significant impact on the integral, which explains the sensitivity against the conditions of the calculation.

3.4 Results assuming a stripping process

As mentioned before, the $^{13}C(\alpha, n)^{16}O$ can also be considered as a stripping mechanism, where an ^3He fragment of the α-particle is transferred to ^{13}C. The entrance and exit-channel potentials are unchanged. The DWBA amplitudes are presented in fig. 6. The agreement between the DWBA and the microscopic model is different according to J. In the non-resonant $3/2^-$ partial wave, both approaches are fairly close to each other. On the contrary, the DWBA provides larger transition amplitudes for $J = 1/2^-$ which involves a broad resonance near 2 MeV. For $J = 1/2^+$, the DWBA strongly underestimates the microscopic approach. As in sect. 3.2, we also use supersymmetric partners of the nucleus-nucleus potentials. The DWBA results

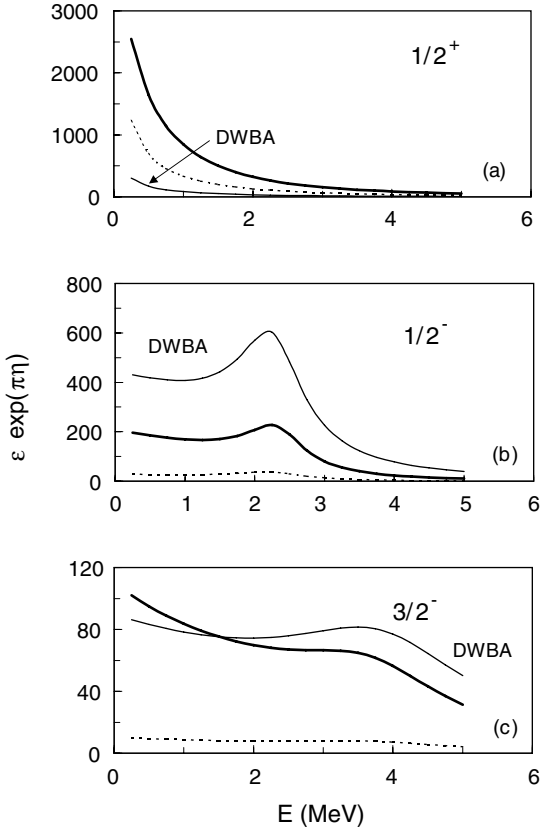

Fig. 6. Transition amplitudes obtained in the stripping approximation for $J = 1/2^+$ (a), $J = 1/2^-$ (b), and $J = 3/2^-$ (c). Thick curve: microscopic reference calculation, thin solid curve: DWBA calculation, dashed curves: DWBA calculation with supersymmetric potentials.

appear to be very sensitive to this choice. Again, the reason is that the DWBA integrand (20) is essentially given by short-distance contributions, which strongly depend on slight details in the wave functions.

4 Conclusion

The aim of the present work is to derive DWBA transition amplitudes, starting from microscopic results. The conditions of the calculation have been chosen to be as equivalent as possible to the microscopic model: the nucleus-nucleus potentials have been fitted to the phase shifts, and the spectroscopic factors are identical. Our example is the $^{13}\mathrm{C}(\alpha, \mathrm{n})^{16}\mathrm{O}$ reaction which is one of the main neutron sources in stars. The DWBA transitions amplitudes have been determined in two assumptions: exchange or stripping processes. In both case, the zero-range approximation has been used; qualitatively this approximation should not affect our results.

The conclusion drawn from this work is twofold. On the one hand, the DWBA method turns out to be very sensitive to the conditions of the calculations: choice of the nucleus-nucleus potentials and, to a lesser extent, of the wave functions of the colliding nuclei. This sensitivity is due to very basic properties, *i.e.* the short-range character of the DWBA matrix elements, which are quite sensitive to details of the wave functions. This is true for broad resonances, but also for non-resonant processes, where the DWBA is expected to be more accurate. On the other hand, the DWBA and the reference microscopic method provide the same energy dependence, as the phase shifts are equivalent. However, the amplitudes can be rather different, and this difference varies with angular momentum. This is most likely due to antisymmetrization effects which are approximately included in the DWBA through the choice of deep nucleus-nucleus potentials. This property should also occur in other systems and suggests that the DWBA method can only provide transfer cross-sections with a non-negligible uncertainty.

Of course, the present comparison relies on some quantities such as V_0 or D_0 which must calculated in a simple way to be as consistent as possible with the GCM. More refined approaches should be used to go beyond this comparison and to apply the DWBA in optimal conditions. However, this does not change the conclusion about the sensitivity of the DWBA to fundamental quantities, such as the wave functions of the colliding nuclei and of the transferred particle. Application of the DWBA to nuclear astrophysics should therefore include this sensitivity in the calculation of the cross-sections.

A.A. thanks the FNRS for financial support. This text presents research results of the Belgian program P5/07 on interuniversity attraction poles initiated by the Belgian-state Federal Services for Scientific, Technical and Cultural Affairs.

References

1. W. Tobocman, *Theory of Direct Nuclear Reactions* (Oxford University Press, New York, 1961).
2. G.R. Satchler, Nucl. Phys. **55**, 1 (1964).
3. T. Tamura, Phys. Rep. **14C**, 59 (1974).
4. G.R. Satchler, *Direct Nuclear Reactions* (Oxford, 1983).
5. D.D. Clayton, *Principles of Stellar Evolution and Nucleosynthesis* (The University of Chicago Press, 1983).
6. G. Raimann, B. Bach, K. Grün, H. Herndl, H. Oberhummer, S. Engstler, C. Rolfs, H. Abele, R. Neu, G. Staudt, Phys. Lett. B **249**, 191 (1990).
7. H. Herndl, H. Abele, G. Staudt, B. Bach, K. Grun, H. Scsribany, H. Oberhummer, G. Raimann, Phys. Rev. C **44**, R952 (1991).
8. T. Rauscher, G. Raimann, Phys. Rev. C **53**, 2496 (1996).
9. S. Kubono, Y. Funatsu, N. Ikeda, M. Yasue, T. Nomura, Y. Fuchi, H. Kawashima, S. Kato, H. Orihara, H. Miyatake, T. Kajino, Z. Phys. A **334**, 511 (1989).
10. N. Keeley, K.W. Kemper, Dao T. Khoa, Nucl. Phys. A **726**, 159 (2003).
11. S. Kubono, K. Abe, S. Kato, T. Teranishi, M. Kurokawa, X. Liu, N. Imai, K. Kumagai, P. Strasser, M.H. Tanaka, Y. Fuchi, C.S. Lee, Y.K. Kwon, L. Lee, J.H. Ha, Y.K. Kim, Phys. Rev. Lett. **90**, 062501 (2003).
12. K. Wildermuth, Y.C. Tang, *A Unified Theory of the Nucleus*, edited by K. Wildermuth, P. Kramer (Vieweg, Braunschweig, 1977).

13. P. Descouvemont, Phys. Rev. C **36**, 2206 (1987).
14. D. Baye, P. Descouvemont, Ann. Phys. (N.Y.) **165**, 115 (1985).
15. J.K. Bair, F.X. Haas, Phys. Rev. C **7**, 1356 (1973).
16. B.K. Barnes, T.A. Belote, J.R. Risser, Phys. Rev. **140**, B616 (1965).
17. K. Langanke, Adv. Nucl. Phys. **21**, 85 (1994).
18. P. Descouvemont, *Proceedings of the International Conference Innovative Computational Methods in Nuclear Many-body Problems, Osaka, Japan (1997)*, edited by H. Horiuchi *et al.* (World Scientific, 1998) p. 205.
19. F. Ajzenberg-Selove, Nucl. Phys. A **564**, 1 (1993).
20. D. Baye, N.K. Timofeyuk, Phys. Lett. B **293**, 13 (1992).
21. T. Rauscher, K. Grün, H. Krauss, H. Oberhummer, E. Kwasniewicz, Phys. Rev. C **45**, 1996 (1992).
22. D. Baye, Phys. Rev. Lett. **58**, 2738 (1987).
23. V.T. Voronchev, V.I. Kukulin, V.N. Pomerantsev, G.G. Ryzhikh, Few-Body Syst. **18**, 191 (1995).
24. D. Baye, P. Descouvemont, M. Kruglanski, Nucl. Phys. A **550**, 250 (1992).